НАУЧНОЕ ИЗДАНИЕ МГТУ ИМ. Н. Э. БАУМАНА

НАУКА и ОБРАЗОВАНИЕ

Эл № ФС77 - 48211. Государственная регистрация №0421200025. ISSN 1994-0408

электронный научно-технический журнал

Анализ косвенного измерения сил резания при точении металлических цилиндрических оболочек

 # 02, февраль 2014

DOI: 10.7463/0214.0687971

Кондратенко К. Е., Гуськов А. М., Гуськов М. А., Лоронг Ф., Пановко Г. Я.

УДК 004.3+519.6

Россия, МГТУ им. Н.Э. Баумана
kirillkondratenko@yandex.ru
gouskov_am@mail.ru
mikhail.guskov@ensam.eu
philippe.lorong@ensam.eu
gpanovko@yandex.ru

Аннотация

Измерение сил резания является важной составляющей разработки и проверки технологических процессов. Использование общепринятых прямых силоизмерительных систем для этой цели часто не представляется возможным. Данная статья предлагает косвенный метод оценки силы резания в процессе обработки точением тонкостенной цилиндрической оболочки. Метод основывается на измерении перемещений гибкой конструкции — детали. Более того, при точении цилиндрических оболочек появляется необходимость использования бесконтактных датчиков перемещений. В данной работе рассматривается конкретная технологическая система, в которой датчики перемещений располагаются вблизи свободного торца цилиндрической оболочки, которая жестко закреплена в патроне токарного станка. Изучается вопрос об измерении двух компонент силы резания — радиальной и окружной. Модель разработана в квази-статическом приближении. Определено оптимальное угловое расположение двух датчиков радиальных перемещений, исходя из условия минимизации числа обусловленности матрицы линейного преобразования, связывающего неизвестные компоненты вектора силы резания с измеряемыми сигналами.

Список литературы

1. Lorong P., Larue A., Duarte A.P. Dynamic Study of Thin Wall Part Turning // Advanced Materials Research. 2011. Vol. 223. P. 591–599. DOI: 10.4028/www.scientific.net/AMR.223.591

2. Герасименко А.А., Гуськов А.М., Гуськов М.А., Лоронг Ф. Определение собственных частот вращающейся цилиндрической оболочки // Инженерный журнал: наука и инновации. 2012. № 6. Режим доступа: http://engjournal.ru/catalog/eng/teormech/262.html (дата 01.01.2014).
3. Fang N., Wu Q. A Comparative Study of the Cutting Forces in High Speed Machining of Ti-6Al-4V and Inconel 718 with a Round Cutting Edge Tool // Journal of Materials Processing Technology. 2009. Vol. 209, no. 9. P. 4385–4389. DOI: 10.1016/j.jmatprotec.2008.10.013
4. Бидерман В.Л. Механика тонкостенных конструкций. М.: Машиностроение, 1977. 488 с.
5. Годунов С.К. О численном решении краевых задач для систем линейных обыкновенных дифференциальных уравнений // Успехи математических наук. 1961. Т. 16, № 3. С. 171–174.
6. Higham N.J. Accuracy and Stability of Numerical Algorithms. 2nd ed. Philadelphia: SIAM. 2002.
7. Householder A.S. Unitary Triangularization of a Nonsymmetric Matrix // Journal of the ACM. 1958. Vol. 5, no. 4. P. 339–342. DOI: 10.1145/320941.320947

SCIENTIFIC PERIODICAL OF THE BAUMAN MSTU

SCIENCE and EDUCATION

EL № FS77 - 48211. №0421200025. ISSN 1994-0408

electronic scientific and technical journal

Analysis of indirectly measured cutting forces in turning metallic cylinder shells

02, February 2014
DOI: 10.7463/0214.0687971

Kondratenko K. E., Gouskov A. M., Guskov M. A., Lorong. P., Panovko G. Ya.

Bauman Moscow State Technical University
105005, Moscow, Russian Federation
kirillkondratenko@yandex.ru
gouskov_am@mail.ru
mikhail.guskov@ensam.eu
philippe.lorong@ensam.eu
gpanovko@yandex.ru

Introduction

In modern manufacturing, cutting forces measurement is a key element in understanding the operational conditions during machining. Nevertheless, in some cases, the use of dynamometers can be problematic, for instance in case of thin-walled workpieces in presence of instabilities: due to the presence of resonances in the frequency response of the dynamometer itself can induce significant perturbations in the measured signals. This was the case for [1]: the addition of the dynamic system of the dynamometer can modify the conditions of the chatter onset.

In the present paper, we address the problem of quasi-static evaluation of the cutting force during turning cylindrical shells. The cutting force components are estimated indirectly, from the displacement measurements, with the help of the flexibility matrix, based on the elastic behavior of the structure.

First, we find the relation between the applied concentrated force components and radial displacements of the points, which radial displacements are actually measured.

Then, the question of the optimality of the sensors position is sought, in terms of the conditioning of the flexibility matrix.

1. Description of the mathematical model

In this section, we develop a quasi-static analysis of the force-displacement relation applied to the case of turning a thin-walled cylindrical shell. The cutting force is taken as concentrated.

Thus, based on the radial displacement measurement by two proximity probes, the sought force components can be expressed by means of the flexibility matrix.

The shell is shown in fig. 1. The left-hand edge of the shell is rigidly fixed, and the right-hand edge is free.

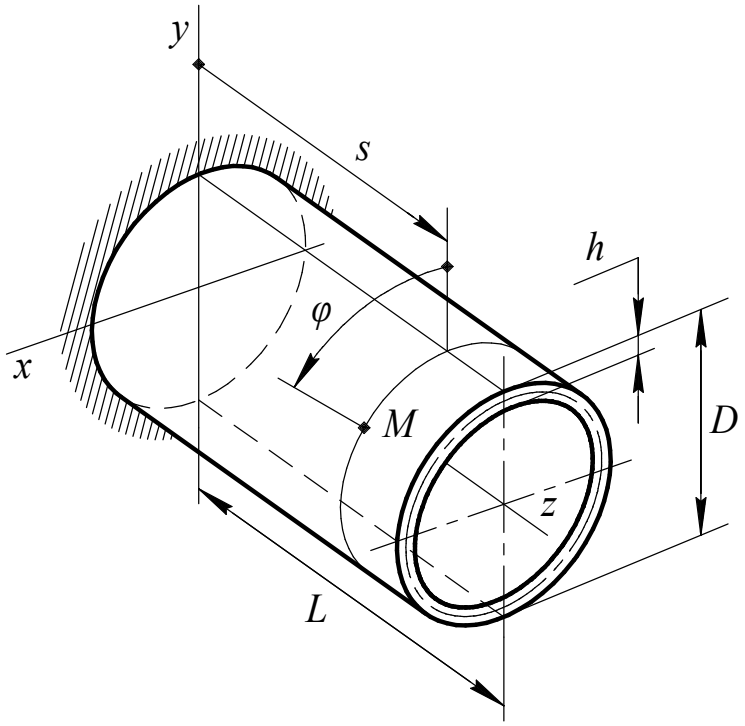

Fig. 1. Shell's dimentions and system of coordinates

In other words, the shell is supported like a cantilever with "clamped-free" boundary conditions. Thickness of the shell is regarded as being much smaller than its diameter: $h \ll D = 2R$. We will be using cylindrical coordinates: axial s and angular φ. An arbitrary point M belonging to the middle surface of the shell is said to have coordinates (s, φ), as shown in fig. 1.

The shell is subjected to pin-load, which is represented by the two components of the cutting force: radial F_R and curcumferential F_C, as shown in Fig. 2. We neglect the axial component of the cutting force because it is always much smaller than the other two components [3], and because the stiffness in the z-direction is much higher than in the other two directions. Forces F_R and F_C act on the point with coordinates $(s_F, 0)$. We introduce Λ as a changeable dimensionless parameter so that $s_F = \Lambda L$, see (fig. 2). We can now write down the expression for the shell's thickness:

$$h(s) = \begin{cases} h_{\text{fin}} \text{if } s < s_F; \\ h_{\text{ini}} \text{if } s \geq s_F. \end{cases} \tag{1}$$

where h_{ini} is the shell's thickness before cutting and h_{fin} is the shell's thickness after cutting.

Now Let us consider the free end of the shell (fig. 3). Two arbitrary points belonging to this end are chosen: point A and point B. The angular location of these points is determined by parameters Φ_1 and Φ_2, which is shown in fig. 3.

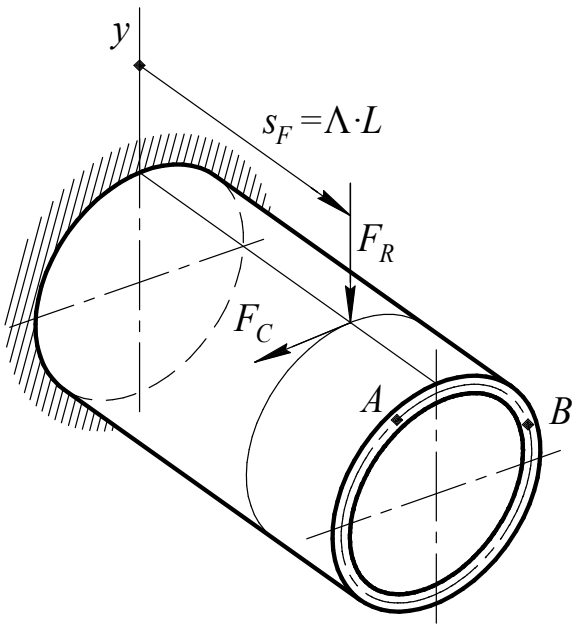

Fig. 2. The components of the cutting force and parameter Λ

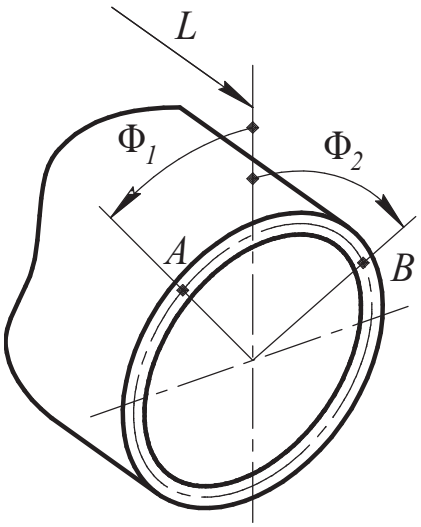

Fig. 3. The free end of the shell. Angular location of the displacement sensors

Forces F_R and F_C, acting on the shell, cause it to deform. Total displacements of points A and B are represented by axial u, circumferential v, and radial w components. In our study we are interested only in radial components of the displacements of the two points since they can be measured using displacement sensors. Since the system we are studying is linear, the relation between the two components F_R, F_C of the cutting force and the radial displacements w_A, w_B of points A and B is naturally expected to be linear and injective (one-to-one):

$$\mathbf{A}\mathbf{f} = \mathbf{e}, \tag{2}$$

where

$$\mathbf{A} = \begin{bmatrix} a_{11} & a_{12} \\ a_{21} & a_{22} \end{bmatrix}, \qquad \mathbf{f} = \begin{bmatrix} F_C \\ F_R \end{bmatrix}, \qquad \mathbf{e} = \begin{bmatrix} w_A \\ w_B \end{bmatrix}. \tag{3}$$

From this moment on we will refer to matrix $\mathbf{A}$ as the flexibility matrix.

The main objective of our work is to estimate the two components of the cutting force (F_C and F_R) given that the radial displacements of the two points A and B, caused by the force, are known. In other words, we are to determine vector $\mathbf{f}$. In order to do that, we will have to calculate the flexibility matrix.

The process of calculation of matrix $\mathbf{A}$ is going to be solely numerical, as we shall see later in this paper. The components of vector $\mathbf{e}$ are measured experimentally, and therefore, subject to measurement errors. In order for the solution $\mathbf{f} = \mathbf{A}^{-1}\mathbf{e}$ to be reliable, system (2) has to be *numerically stable*. Because of these reasons, not only do we have to calculate matrix $\mathbf{A}$, which is addressed in Section 2, but we also have to ensure its numerical stability, which will be discussed later in this paper. The question of numerical stability of the flexibility matrix is addressed in Section 3.

Given that the shell's geometry and material properties are not subject to variation, it is apparent that the components of matrix $\mathbf{A}$ are dependant on the three variable parameters that we have introduced earlier: $\mathbf{A} = \mathbf{A}(\Phi_1, \Phi_2, \Lambda)$.

2. Calculation of the flexibility matrix

According to [4], the general system of equations for a Kirchhoff-Love thin-walled cylindrical shell, which is shown in Fig. 1, can be written in the following form

$$\begin{cases} \dfrac{\partial u}{\partial s} = \dfrac{1-\nu^2}{Eh} T_1 - \dfrac{\nu}{R}\Big(\dfrac{\partial v}{\partial \varphi} + w\Big), \\ \dfrac{\partial v}{\partial s} = \dfrac{2(1+\nu)}{Eh} S_1^* - \dfrac{h^2}{3R^2}\dfrac{\partial \theta_1}{\partial \varphi} + \Big(\dfrac{h^2}{3R^3} - \dfrac{1}{R}\Big)\dfrac{\partial u}{\partial \varphi}, \\ \dfrac{\partial w}{\partial s} = -\theta_1, \\ \dfrac{\partial \theta_1}{\partial s} = \dfrac{12(1-\nu^2)}{Eh^3} M_1 + \dfrac{\nu}{R^2}\Big(\dfrac{\partial^2 w}{\partial \varphi^2} - \dfrac{\partial v}{\partial \varphi}\Big), \\ \dfrac{\partial}{\partial s}(RT_1) = -\dfrac{\partial S_1^*}{\partial \varphi} + \dfrac{Eh^3}{6R^2(1+\nu)}\Big(\dfrac{\partial^2 \theta_1}{\partial \varphi^2} - \dfrac{\partial^2 u}{\partial R \partial \varphi^2}\Big) - Rq_1, \\ \dfrac{\partial}{\partial s}(RS_1^*) = -\dfrac{\nu}{R}\dfrac{\partial M_1}{\partial \varphi} - \dfrac{Eh^3}{12R^3}\Big(\dfrac{\partial^2 v}{\partial \varphi^2} - \dfrac{\partial^3 w}{\partial \varphi^3}\Big) - \nu\dfrac{\partial T_1}{\partial \varphi} - \dfrac{Eh}{R}\Big(\dfrac{\partial^2 v}{\partial \varphi^2} + \dfrac{\partial w}{\partial \varphi}\Big) - Rq_2, \\ \dfrac{\partial}{\partial s}(RQ_1^*) = -\dfrac{\nu}{R}\dfrac{\partial^2 M_1}{\partial \varphi^2} - \dfrac{Eh^3}{12R^3}\Big(\dfrac{\partial^3 v}{\partial \varphi^3} - \dfrac{\partial^4 w}{\partial \varphi^4}\Big) + \nu T_1 + \dfrac{Eh}{R}\Big(\dfrac{\partial v}{\partial \varphi} + w\Big) - Rq_3, \\ \dfrac{\partial}{\partial s}(RM_1) = \dfrac{Eh^3}{6R(1+\nu)}\Big(\dfrac{\partial^2 u}{\partial R \partial \varphi^2} - \dfrac{\partial^2 \theta_1}{\partial \varphi^2}\Big) + RQ_1^*. \end{cases}$$

where E is the Young modulus, ν is the Poisson's ratio, h is the shell's wall-thickness, R is the shell's radius, u is the axial direction displacement, v is the circumferential direction displacement, w is the radial direction displacement, θ_1 is the surface normal's angular displacement, T_1, S_1^*, Q_1^*, M_1 are the internal forces, and q_1, q_2, q_3 represent the external loading. This is a linear system of partial differential equations that may also be written in form

$$\mathbf{L}\mathbf{y} = \mathbf{g}, \tag{4}$$

where $\mathbf{L}$ is a linear partial differential operator represented by (8×8) matrix and vector $\mathbf{y}$ is the state vector:

$$\mathbf{y} = (u,\ v,\ w,\ \theta_1,\ RT_1,\ RS_1^*,\ RQ_1^*,\ RM_1)$$

and vector $\mathbf{g}$ is the load vector:

$$\mathbf{g} = -R \cdot (0,\ 0,\ 0,\ 0,\ q_1,\ q_2,\ q_3,\ 0).$$

System (4) belongs to the so-called class of separable systems, which means that it is possible to separate variables s and φ with the aid of the Fourier method using complex Fourier series:

$$\mathbf{y} = \sum_{k=-\infty}^{+\infty} \mathbf{y}_{(k)} \cdot \exp(ik\varphi). \tag{5}$$

Vector $\mathbf{y}_{(k)}$ depends only on variable s and is called the k-th harmonic of vector $\mathbf{y}$. After separation of variables, system (4) is decomposed into the infinite amount of linear 8-th order systems of ordinary differential equations (ODE). Each of these ODE systems can be written in matrix notation as follows

$$\frac{d}{ds}\,\mathbf{y}_{(k)} = \mathbf{F}_{(k)}\,\mathbf{y}_{(k)} + \mathbf{g}_{(k)}, \tag{6}$$

where $\mathbf{F}_{(k)}$ is (8×8) constant square matrix:

$$\mathbf{F}_{(k)} = \begin{bmatrix} 0 & -\frac{i\nu k}{R} & -\frac{\nu}{R} & 0 & \frac{1-\nu^2}{EhR} & 0 & 0 & 0 \\ -\frac{ik}{R} & 0 & 0 & 0 & 0 & \frac{2(1+\nu)}{EhR} & 0 & 0 \\ 0 & 0 & 0 & -1 & 0 & 0 & 0 & 0 \\ 0 & -\frac{i\nu k}{R^2} & -\frac{\nu k^2}{R^2} & 0 & 0 & 0 & 0 & \frac{12(1-\nu^2)}{Eh^3R} \\ \frac{A}{R^2} & 0 & 0 & -\frac{A}{R} & 0 & -\frac{ik}{R} & 0 & 0 \\ 0 & \frac{Ehk^2}{R} & -B & 0 & -\frac{i\nu k}{R} & 0 & 0 & -\frac{i\nu k}{R^2} \\ 0 & B & C & 0 & \frac{\nu}{R} & 0 & 0 & \frac{\nu k^2}{R^2} \\ -\frac{A}{R} & 0 & 0 & A & 0 & 0 & 1 & 0 \end{bmatrix}$$

where

$$A = \frac{Eh^3k^2}{6R(1+\nu)}, \qquad B = \frac{iEhk}{R}\Big(1 + \frac{h^2k^2}{12R^2}\Big), \qquad C = \frac{Eh}{R}\Big(1 + \frac{h^2k^4}{12R^2}\Big).$$

We can formally express the concentrated cutting force as a distributed load using the Dirac delta function. Keeping in mind that $\dim \delta(x) = 1/\dim x$, it is quite obvious that

$$(q_1,\ q_2,\ q_3) = (0,\ F_C,\ -F_R) \cdot \frac{\delta(\varphi)\,\delta(s - s_F)}{R}.$$

Using the Fourier series of the Dirac delta function

$$\delta(\varphi) = (2\pi)^{-1} \sum_{k=-\infty}^{+\infty} \exp(ik\varphi),$$

the load vector can be rewritten as

$$\mathbf{g}_{(k)} = \frac{1}{2\pi}(0,\ 0,\ 0,\ 0,\ 0,\ -F_C,\ F_R,\ 0)\,\delta(s - s_F).$$

The left end of the shell ($s = 0$) is rigidly fixed, and the right end ($s = L$) is free. The followings are the boundary conditions:

$$\begin{aligned} &\big(u_{(k)},\ v_{(k)},\ w_{(k)},\ \theta_{1(k)}\big) = 0 \ \text{ at } s = 0; \\ &\big(RT_{1(k)},\ RS^*_{1(k)},\ RQ^*_{1(k)},\ RM_{1(k)}\big) = 0 \ \text{ at } s = L. \end{aligned} \tag{7}$$

Here are the continuity conditions at point ($s = s_F$):

$$\mathbf{y}_{(k)}(s_F + \varepsilon) = \mathbf{y}_{(k)}(s_F - \varepsilon) + \frac{1}{2\pi}(0,\ 0,\ 0,\ 0,\ 0,\ -F_C,\ F_R,\ 0),$$

where ε is an infinitesimally small parameter.

System (6) along with boundary conditions (7) represent a boundary value problem. We have used the initial parameters method [4] in order to solve this problem by means of numerical integration. The Godunov orthogonalization method [5] was incorporated to ensure numerical stability of the solution. Moreover, the method was further modified in order to eliminate the well-known Gram-Schmidt process's weakness [6]. The Gram-Schmidt process was replaced by the Householder transformation [7], which effectively performs the same thing — orthonormalizes a set of vectors in the Euclidean space $\mathbb{R}^n$.

Harmonic $w_{(k)}(L)$ that corresponds to the radial displacements of points located on the free end of the shell, can be represented as a linear combination of the cutting force components:

$$w_{(k)}(L) = F_C \cdot \alpha_{(k)} + F_R \cdot \beta_{(k)},$$

where coefficients $\alpha_{(k)}$ and $\beta_{(k)}$ depend only on parameter Λ and have been obtained after numerical integration of the boundary value problem for different harmonics. According to expression (5),

$$w(L, \varphi) = \sum_{k=-\infty}^{+\infty} \left(F_C\, \alpha_{(k)} + F_R\, \beta_{(k)}\right) \exp\left(ik\varphi\right).$$

According to the definition (see fig. 3), we can write that $w_A = w(L, \Phi_1)$ and $w_B = w(L, -\Phi_2)$. Finally, according to formulas (2) and (3), matrix $\mathbf{A}$ can be represented as an infinite series

$$\mathbf{A} = \sum_{k=-\infty}^{+\infty} \begin{bmatrix} \alpha_{(k)} \exp\left(ik\Phi_1\right) & \beta_{(k)} \exp\left(ik\Phi_1\right) \\ \alpha_{(k)} \exp\left(-ik\Phi_2\right) & \beta_{(k)} \exp\left(-ik\Phi_2\right) \end{bmatrix}.$$

It can be shown that the components of matrix $\mathbf{A}$ are always real numbers, which they must be, of course, since $\mathbf{A}$ is the flexibility matrix.

Table. 1 shows the number of harmonics that we have had to take into account in order to meet ε-accuracy. The criteria of meeting the required accuracy has been

$$\|\mathbf{A}_{N+5} - \mathbf{A}_N\| \cdot \|\mathbf{A}_N\|^{-1} \leq \varepsilon.$$

Table 1

Number of harmonics N corresponding to relative accuracy ε

ε	0.1	0.01	0.001	0.0001
N	10	17	25	32

If the above inequality is satisfied, then we consider approximation $\mathbf{A}_N$ to be accurate enough. Note that table. 1 represents approximate numbers of harmonics, since these numbers depend not only on ε, but also on Λ, Φ_1 and Φ_2. In our work, we have set the relative accuracy to $\varepsilon = 0.01 = 1\%$.

Now that we know how to calculate matrix $\mathbf{A}$, we can estimate the order of magnitude of the displacements. The magnitude of the cutting force is approximately 10^2–10^3 N, according to [3]. Using this data and our model, we have calculated that magnitudes of the displacements are within 10^{-5} m.

3. Optimization of the displacement sensors location

We need to determine the best set of parameters Φ_1 and Φ_2 (the displacement sensors angular location) that would make the system (2) as well-conditioned as possible. A measure of a square matrix's numerical stability is called its condition number μ. By definition [6],

$$\mu(\mathbf{A}) = \|\mathbf{A}\| \cdot \|\mathbf{A}^{-1}\|.$$

Condition number μ is always a positive number, and it cannot be less than one. The closer the condition number μ of the flexibility matrix $\mathbf{A}$ is to one, the more well-conditioned this matrix is. Therefore, to ensure the best numerical stability of the linear transformation (2) we must minimize the condition number μ of matrix $\mathbf{A}$. Let us construct the target function:

$$f(\Phi_1, \Phi_2) = \max_{\Lambda} \Big[\mu\big(\mathbf{A}(\Phi_1, \Phi_2, \Lambda)\big)\Big]. \tag{8}$$

To accomplish our optimization goal we have to minimize f:

$$f \to \min.$$

We have implemented the brute force approach minimizing function f. Angular increment has been set to $0.1°$, and the increment for parameter Λ has been set to 0.05. Color plot of function $\mu^{-1}\big(\mathbf{A}(\Phi_1, \Phi_2, 1)\big)$ is shown in fig. 4.

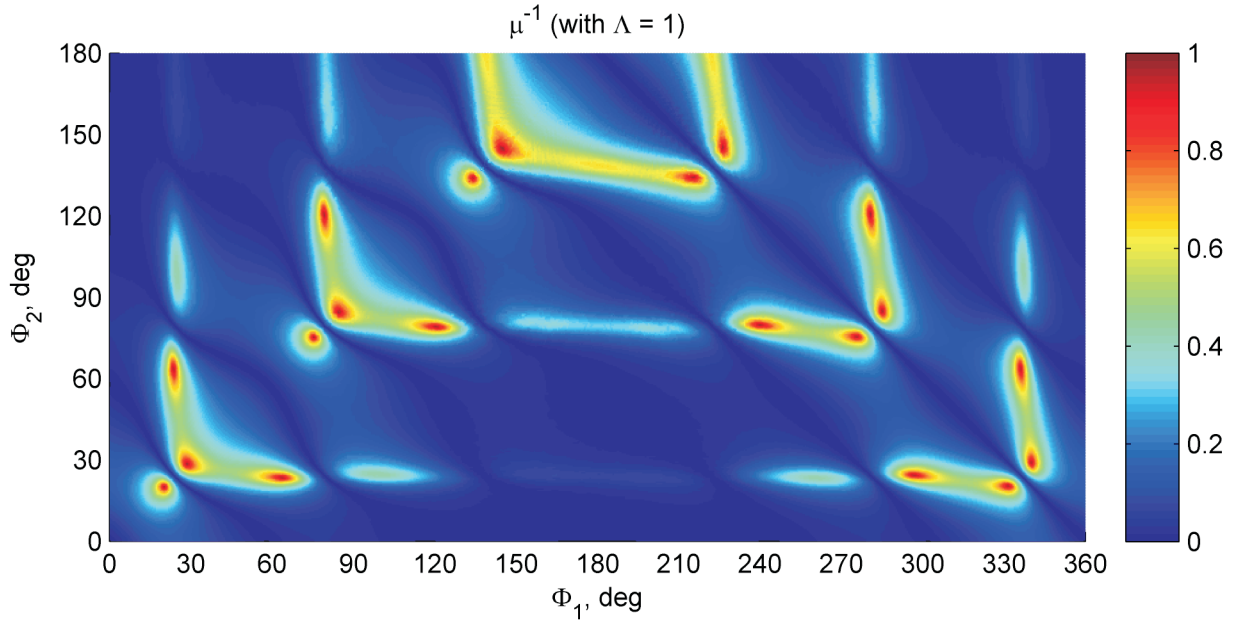

Fig. 4. Color plot of inverse condition number $\mu^{-1}(\mathbf{A})$ with $\Lambda = 1$

We have chosen to analyze function inverse to the condition number because this function is normalized: its range of values lies inside interval $(0,\ 1)$. The diargram features 20 major local maxima (see Table 2). The best choice of parameters is $\Phi_1 = \Phi_2 = 20.4°$, which corresponds to the target function value of 1.2.

Strictly speaking, this value is the global minimum of function $f(\Phi_1, \Phi_2)$. However, in practical terms, any of the displacement sensors configurations from Tables 2 and 3 can be chosen because magnitude of f for any of those configurations does not even exceed 10.

Table 2

Local extrema of f

Code	Φ_1	Φ_2	f
AS	20.4°	20.4°	1.2
BS	30.6°	30.6°	1.5
C1	66.6°	24.3°	1.5
C2	24.3°	66.6°	1.5
DS	77.7°	77.7°	2.8
ES	89.3°	89.3°	1.9
F1	119.4°	83.5°	2.4
F2	83.5°	119.4°	2.4
GS	136.2°	136.2°	2.7
HS	149.5°	149.5°	1.7

Table 3

Local extrema of f

Code	Φ_1	Φ_2	f
I1	208.3°	137.5°	1.8
I2	222.5°	151.7°	1.8
J1	241.1°	83.5°	2.0
J2	276.5°	119.9°	2.0
K1	268.5°	78.6°	2.0
K2	281.5°	91.5°	2.0
L1	293.5°	25.3°	1.4
L2	334.7°	66.5°	1.4
M1	329.3°	20.5°	1.2
M2	339.5°	30.7°	1.2

It means that at the worst case scenario we could lose 1–2 significant digits [6] calculating the components of the cutting force using equation (2), which corresponds to relative accuracy $\varepsilon = 10^{-10}$. Such loss is not significant in comparison with other sources of error in our model. Four most preferable symmetrical displacement sensors configurations are shown in fig. 5, 6, 7 and 8. In these figures, the free end of the shell is shown and the displacement sensors angular locations correspond to fig. 3.

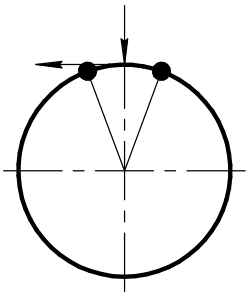

Fig. 5. Conf. AS. $\Phi_1 = \Phi_2 = 20.4°$

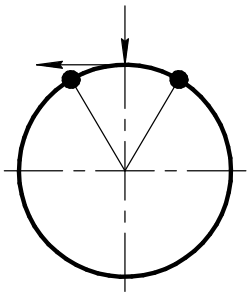

Fig. 6. Conf. BS. $\Phi_1 = \Phi_2 = 30.6°$

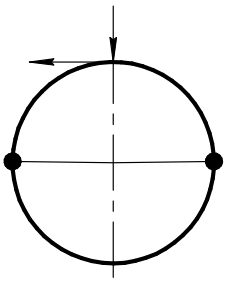

Fig. 7. Conf. ES. $\Phi_1 = \Phi_2 = 20.4°$

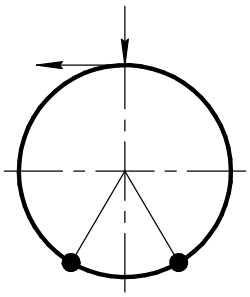

Fig. 8. Conf. HS. $\Phi_1 = \Phi_2 = 30.6°$

Conclusions

In this work we have developed a mathematical model in order to be able to calculate the flexibility matrix that makes it possible to estimate the cutting force components based on displacement measurement in turning cylindrical shells. Analysis of the behavior of the flexibility matrix condition number has been performed. Based on this analysis, optimal configurations of the displacement sensors location have been suggested. These configurations make the flexibility matrix well-conditioned and the process of calculating the components of the cutting force numerically stable.

References

1. Lorong P., Larue A., Duarte A.P. Dynamic Study of Thin Wall Part Turning. *Advanced Materials Research*, 2011, vol. 223, pp. 591–599. DOI: 10.4028/www.scientific.net/AMR.223.591
2. Gerasimenko A.A., Gus'kov A.M., Gus'kov M.A., Lorong F. Opredelenie sobstvennyh chastot vrashchajushchejsja tsilindricheskoj obolochki [Determination of rotating cylindrical shell natural frequencies]. *Inzhenernyy vestnik MGTU im. N.E. Baumana* [Engineering Herald of the Bauman MSTU], 2012, no. 6. Available at: http://engjournal.ru/catalog/eng/teormech/262.html, accessed 01.01.2014. (In Russian)
3. Fang N., Wu Q. A Comparative Study of the Cutting Forces in High Speed Machining of Ti-6Al-4V and Inconel 718 with a Round Cutting Edge Tool. *Journal of Materials Processing Technology*, 2009, vol. 209, no. 9, pp. 4385–4389. DOI: 10.1016/j.jmatprotec.2008.10.013
4. Biderman V.L. Mekhanika tonkostennykh konstruktsiy [Mechanics of thin-walled structures]. Moscow, Mashinostroenie, 1977. 488 p. (In Russian)
5. Godunov S.K. [Numerical solution of boundary-value problems for systems of linear ordinary differential equations]. *Uspekhi matematicheskikh nauk*, 1961, vol. 16, no. 3, pp. 171–174. (In Russian)
6. Higham N.J. Accuracy and Stability of Numerical Algorithms. 2nd ed. Philadelphia, SIAM. 2002.
7. Householder A.S. Unitary Triangularization of a Nonsymmetric Matrix. *Journal of the ACM*, 1958, vol. 5, no. 4, pp. 339–342. DOI: 10.1145/320941.320947